Fifth International Conference on CFD in the Process Industries
CSIRO, Melbourne, Australia
13-15 December 2006

A COMBINED METHOD FOR SIMULATING GAS-PARTICLE FLOWS IN HIGHLY LADEN CYCLONES

Stefan PIRKER, Damir KAHRIMANOVIC

[1] Johannes Kepler University, Altenbergerstr. 69, A-4040 Linz, AUSTRIA

ABSTRACT

If the mass loading of a cyclone increases, particle-particle interactions start playing a dominant role. Eventually, a particle strand is formed in the outer region of the cyclone that is responsible for most of the particle collection.

In this paper a combined Euler-Euler granular and Euler-Lagrange simulation approach is presented. While the particle strand is governed by a continuous kinetic theory the particles in the dilute inner region are traced in a Lagrangian frame of reference. The combination of the two well known models is organized in four steps. First, (a) based on a mono-disperse Euler-Euler granular simulation the free shear layer of the particle strand is identified. Next, (b) distinct poly-disperse particles are emitted into the dilute surroundings. Those particles are (c) traced until they (d) escape by the cyclone outlet or re-enter the particle strand.

The above hybrid model is tested for a high-throughput cyclone and results of the collection efficiency are compared with analytical results.

NOMENCLATURE

$\mathbf{A}_{\mathbf{c}\perp\mathbf{RSL}}$	cell's RSL-area vector
C_D^*	drag coefficient for particles
$D_{t,g}$	gas phase turbulent diffusion coefficient
d_s	particle diameter
e_{ss}	coefficient of restitution for particle collisions
$\mathbf{F}_{\mathbf{D,s}}$	particle drag force
g	gravitational acceleration
$g_{0,ss}$	radial distribution function
$\mathbf{I}$	unit matrix
K_{sg}	gas-solid exchange coefficient
$k_{g,dilute}$	specific energy of the gaseous turbulent fluctuations
m_s	mass of the particulate phase
$N_{Sc,t}$	turbulent Schmidt-number
p	pressure shared by all phases
p_s	granular pressure
Re_s	particle Reynolds-number
$\mathbf{S}_\mathbf{g}$	strain rate tensor
S_s	mass source for the particulate phase
$\mathbf{u}_\mathbf{g}$	gas velocity
$\mathbf{u}_\mathbf{s}$	velocity of particulate phase
$\mathbf{u}_{\mathbf{s,strand}}$	mean particle strand velocity
u_τ	shear stress velocity
$v_{r,s}$	terminal particle velocity
α_g	gas phase volume fraction
α_s	particulate phase volume fraction
Θ_s	granular temperature
$\mu_{eff,g}$	gas phase effective viscosity
μ_g	gas phase viscosity
$\mu_{s,bulk}$	granular bulk viscosity
$\mu_{s,coll}$	granular phase collisional viscosity
$\mu_{s,kin}$	granular phase kinetic viscosity
$\nu_{t,g}$	gas phase turbulent kinematic viscosity
ρ_g	gas density
ρ_s	density of particulate phase
$\boldsymbol{\tau}_\mathbf{g}$	gas phase stress tensor
$\boldsymbol{\tau}_{RSM,g}$	gas phase Reynolds stresses tensor
$\boldsymbol{\tau}_\mathbf{s}$	particulate phase stress tensor

INTRODUCTION

For the simulation of particulate flows two main approaches are in common use. First, distinct particles can be traced in a Lagrangian way through a velocity field that is based on an Eulerian locally fixed grid. In the second approach the multitude of particles is considered as an additional continuous phase. Thus, individual particles properties and behaviour are smeared out and described in an Eulerian frame of reference. While the first approach is known as Euler-Lagrange (EuLa) or discrete particle method the second is called two fluid or Euler-Euler (EuEu) method.

Both methods have their pros and contras. The EuLa model (e.g. Sommerfeld, 1996) is intuitively understandable and physically straight forward but it is somehow difficult to consider particle-particle interactions particularly if many particles are involved. Thus, in most commercial codes the standard EuLa model neglects particle-particle interactions.
On the other hand EuEu models can account for particle-particle interactions by introducing granular quantities like

pressure, temperature or viscosity that can be deduced from kinetic theory (e.g. Gidaspow, 1994). Nevertheless, modelling uncertainties are very hard to estimate and the computational costs for solving the additional transport equations are very high especially if more particle classes are involved.

Therefore, it is an obvious attempt to combine these two approaches in order to benefit from their individual strengths. This combining approach is known from avalanche modelling (e.g. Zwinger, 2000) and in this paper a modified model is applied for the simulation of highly laden cyclones. For sake of clarity this combination is called Euler-Euler-Lagrange (EuEuLa) model.

In highly laden cyclones a particle strand is formed at the outer wall that can be distinguished from a dilute inner core region. Linking the cyclone flow to the snow flow modelling the particle strand would represent the dense avalanche layer and the inner core region would stand for the snow crystal laden atmosphere.

The next three sections are dedicated to the description of the basic models namely the EuEu, the EuLa and the combining EuEuLa model. Afterwards, a highly laden cyclone is considered as an application and first numerical results are presented.

MODELING I - EULER-EULER-GRANULAR SIMULATIONS

In the Euler-Euler (EuEu) approach particles are assumed as a continuous phase that can interpenetrate the gaseous phase. Thus, a whole set of Navier-Stokes equations is applied for both the continuous gas phase and the particulate phase. Thereby, both phases are described by an unique velocity field but share a common pressure field.

The mass conservation reads for the gas phase

$$\frac{\partial}{\partial t}\left(\alpha_g \rho_g\right)+\nabla\cdot\left(\alpha_g \rho_g \mathbf{u_g}\right)=0 \tag{1}$$

and for the particulate phase

$$\frac{\partial}{\partial t}\left(\alpha_s \rho_s\right)+\nabla\cdot\left(\alpha_s \rho_s \mathbf{u_s}\right)=S_s\,. \tag{2}$$

In above equations α denotes the volume fraction of the very phase with

$$\alpha_g+\alpha_s=1. \tag{3}$$

In the mass conservation of the particulate phase a mass sink S_s is introduced in order to model the particle collection at the lower cyclone outlet.

The momentum conservation for the gas phase is represented by

$$\begin{aligned}\frac{\partial}{\partial t}\left(\alpha_g \rho_g \mathbf{u_g}\right)+\nabla\cdot\left(\alpha_g \rho_g \mathbf{u_g}\mathbf{u_g}\right)=&-\alpha_g\nabla p+\\ &\nabla\cdot\boldsymbol{\tau}_\mathbf{g}+\alpha_g\rho_g\mathbf{g}+K_{sg}\left(\mathbf{u_s}-\mathbf{u_g}\right)\end{aligned} \tag{4}$$

In above equation the instantaneous and convective acceleration is equalled by forces due to pressure gradients, viscous and buoyant forces as well as forces due to the interpenetrating particulate phase. Thereby, the gas stress tensor $\boldsymbol{\tau_g}$ comprises molecular and turbulent Reynolds stresses. The latter Reynolds stresses have to be modelled by an appropriate turbulence model as addressed later.

$$\boldsymbol{\tau}_\mathbf{g}=\alpha_g\mu_g\left(\nabla\mathbf{u_g}+\left(\nabla\mathbf{u_g}\right)^T\right)+\boldsymbol{\tau}_{RSM,g} \tag{5}$$

The last term in equation (4) describes the drag force of the particulate phase acting on the gas phase with

$$K_{sg}=\frac{3\alpha_s\alpha_g\rho_g}{4v_{r,s}^2 d_s}C_D\left(\frac{\mathrm{Re}_s}{v_{r,s}}\right)\left|\mathbf{u_s}-\mathbf{u_g}\right| \tag{6}$$

as a gas-solid exchange coefficient (Syamlal, 1989). The drag coefficient can be described by Dalla Valle (1948)

$$C_D=\left(0.63+\frac{4.8}{\sqrt{\mathrm{Re}_s/v_{r,s}}}\right) \tag{7}$$

with the particle based Reynolds number

$$\mathrm{Re}_s=\frac{\rho_g d_s\left|\mathbf{u_s}-\mathbf{u_g}\right|}{\mu_g} \tag{8}$$

and the terminal particle velocity

$$\begin{aligned}v_{r,s}=&\frac{1}{2}\left(A-0.06\,\mathrm{Re}_s+\right.\\ &\left.\sqrt{\left(0.06\,\mathrm{Re}_s\right)^2+0.12\,\mathrm{Re}_s\left(2B-A\right)+A^2}\right)\end{aligned} \tag{9}$$

The coefficients A and B are detailed in Garside (1977).

The momentum conservation for the particulate phase can be written as

$$\begin{aligned}\frac{\partial}{\partial t}\left(\alpha_s \rho_s \mathbf{u_s}\right)+\nabla\cdot\left(\alpha_s \rho_s \mathbf{u_s}\mathbf{u_s}\right)=&-\alpha_s\nabla p\\ -\nabla p_s+\nabla\cdot\boldsymbol{\tau}_\mathbf{s}+\alpha_s\rho_s\mathbf{g}&+K_{gs}\left(\mathbf{u_g}-\mathbf{u_s}\right)+\mathbf{S_s}\end{aligned} \tag{10}$$

In above equation the granular pressure needs further modelling

$$p_s=\alpha_s\rho_s\Theta_s+2\rho_s\left(1+e_{ss}\right)\alpha_s^2 g_{0,ss}\Theta_s \tag{11}$$

with Θs denoting the granular temperature as a measure for the energy of the particle velocity fluctuations that can be derived by an algebraic expression (Syamlal, 1993). The restitution coefficient e_{ss} describes momentum losses during particle collisions and is set to 0.9. Finally, the radial distribution function is chosen as

$$g_{0,ss}=\left(1-\left(\frac{\alpha_s}{\alpha_{s,\max}}\right)^{\frac{1}{3}}\right)^{-1} \tag{12}$$

Neglecting frictional effects the shear stresses for the solid phase can be described by

$$\begin{aligned}\boldsymbol{\tau}_\mathbf{s}=&\left(\mu_{s,kin}+\mu_{s,coll}\right)\left(\nabla\mathbf{u_s}+\left(\nabla\mathbf{u_s}\right)^T\right)\\ &-\mu_{s,bulk}\left(\nabla\cdot\mathbf{u_s}\right)\mathbf{I}\end{aligned} \tag{13}$$

with the kinetic viscosity

$$\begin{aligned}\mu_{s,kin}=&\frac{\alpha_s d_s \rho_s\sqrt{\Theta_s\pi}}{6\left(3-e_{ss}\right)}\\ &\left[1+\frac{2}{5}\left(1+e_{ss}\right)\left(3e_{ss}-1\right)\alpha_s g_{0,ss}\right],\end{aligned} \tag{14}$$

the collisional viscosity

$$\mu_{s,coll}=\frac{4}{5}\alpha_s\rho_s d_s g_{0,ss}\left(1+e_{ss}\right)\left(\frac{\Theta_s}{\pi}\right)^{1/2}, \tag{15}$$

as well as the granular bulk viscosity

$$\mu_{s,b} = \frac{4}{3}\alpha_s \rho_s d_s g_{0,ss}(1+e_{ss})\left(\frac{\Theta_s}{\pi}\right)^{1/2}. \quad (16)$$

In cyclone operation the turbulence structure is known to be highly anisotropic. Therefore, a modified Reynolds Stress Model (RSM) is applied for the gas-solid mixture (Slack, 2003). In this approach a total amount of eight transport equations is considered for the six independent Reynolds stresses, the turbulent kinetic energy and the dissipation rate. Thus, the gas and solid phase share a common turbulence field. Nevertheless, as the interactions between the particle movement and the continuous phase turbulent fluctuations is yet not fully understood this approach should be considered with caution.

All in all a set of 15 transport equations is solved for a basic three-dimensional, mono-disperse EuEu simulation. Every further particle class would add four transport equations. Thus, a EuEu simulation of cyclone separation of several particle classes quickly tends to be unaffordable.

MODELING II – DISCRETE EULER-LAGRANGE SIMULATIONS

In the second common basic approach only the gas phase is treated as a continuum while the distinct parcels of particles are traced in a Lagrangian frame of reference. Therefore, this model is called discrete particle or Euler-Lagrange (EuLa) model.

In the EuLa model a simplified set of incompressible Navier-Stokes equations is solved for the gas phase consisting of mass

$$\nabla \cdot \mathbf{u_g} = 0, \quad (17)$$

and momentum conservation

$$\frac{\partial}{\partial t}\left(\rho_g \mathbf{u_g}\right) + \nabla \cdot \left(\rho_g \mathbf{u_g}\mathbf{u_g}\right) = -\nabla p + \nabla \cdot \boldsymbol{\tau}_\mathbf{g} + \mathbf{F_{D,s}}. \quad (18)$$

In above equation the stress tensor once again comprises molecular viscous stresses and the Reynolds stresses stemming from the gas phase RSM model. The momentum source due to the drag force of the particles $\boldsymbol{F_{D,s}}$, is monitored and accumulated in every cell the distinct particles pass by.

The trajectories of the particles are calculated based on the gas-phase velocity field by evaluation of a local momentum balance

$$\frac{d}{dt}\mathbf{u}_s = \frac{18\,\mu_g}{\rho_s d_s^2}\frac{C_D^* \,\mathrm{Re}_s}{24}\left(\mathbf{u_g} - \mathbf{u_s}\right) + \mathbf{g}. \quad (19)$$

In above equation the acceleration of the particle is caused by its drag force and the gravitational acceleration. The drag coefficient can be further detailed by

$$C_D^* = A + \frac{B}{\mathrm{Re}_s} + \frac{C}{\mathrm{Re}_s^2}, \quad (20)$$

with coefficients A, B and C that can be found in (Morsi and Alexander, 1972).
All in all using the EuLa model a total of 12 transport equations has to be solved. An additional particle class can be added without the need of a further transport equation. Thus, considering different particle classes the EuLa model is by far cheaper than the EuEu model.

The big draw-back of the standard EuLa model is that particle-particle interactions are not accounted for. Therefore, important phenomena like dense particle separation in cyclones cannot be handled by this model. Therefore, the EuLa model is not appropriate in the case of highly laden gas-solid cyclones.

MODELING III – COMBINED SIMULATIONS

In the preceding sections the advantages and draw-backs of the two main simulation approaches were outlined. If these models are combined advantageous synergy effects can be achieved.

On principal a description of the physical coupling mechanism between a particle strand regime that is dominated by the physics of particle-particle interaction and an outer dilute gas domain can be found in literature on the modelling of snow avalanches (e.g. Zwinger, 2000).

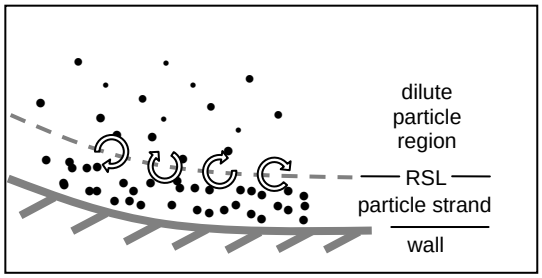

Figure 1: Schematic description of the RSL model.

Thereby, a re-suspension layer (RSL) is assumed to exist in between the dense particle region and the dilute outer region. While physically no sharp boundary exists between these regions it is somehow defined at a particle volume fraction of α_s= 0.01.

Across this RSL particle transport occurs due to turbulent fluctuations as sketched in Figure 1. Applying Reynolds analogy this diffusive particle transport can be linked to the gaseous turbulent momentum diffusion by a turbulent Schmidt number.

$$N_{Sc.t} = \frac{\nu_{t,g}}{D_{t,g}} \cong 1 \quad (21)$$

Next, in a general three-dimensional stress situation a representative shear stress velocity can be deduced from the strain rate tensor $\boldsymbol{S_g}$ by the square root of the second tensor invariant

$$u_{\tau,g} = \sqrt{\nu_{t,g}\sqrt{\frac{1}{2}\,\mathbf{S_g} : \mathbf{S_g}}} \quad (22)$$

Once the shear stress velocity is modelled the corresponding mass flux can be evaluated as

$$\frac{d\,m_s}{dt} = \rho_s \frac{u_{\tau,g}}{N_{Sc,t}}\,\Delta\alpha_s \cdot \mathbf{A_{c\perp RSL}} \quad (23)$$

In above equation $\mathbf{A_{c,RSL}}$ is the cell's RSL-area vector pointing from the particle strand towards the dilute region. The diffusive particle transport across the RSL is driven by a local particle concentration difference $\Delta\alpha_s$. The

initial velocity of the particles is assumed normal to the RSL and its magnitude is set to

$$\mathbf{u}_s = \mathbf{u}_{s,strand} + \zeta \sqrt{\frac{2\,k_{g,dilute}}{3}} \cdot \frac{\mathbf{A}_{c\perp RSL}}{|\mathbf{A}_{c\perp RSL}|} \qquad (24)$$

In above equation $\boldsymbol{u}_{s,strand}$ denotes the mean particle velocity in the neighbouring particle strand cell, ζ represents a random number between 0 and 1 and k_g is the specific energy of the gaseous turbulent fluctuations in the neighbouring dilute region's cell.

At each RSL position the emitting particle diameters are set in accordance with the initial particle spectrum. Thus, at the RSL of a particle strand that is based on a mono-disperse EuEu simulation poly-disperse particles are released.

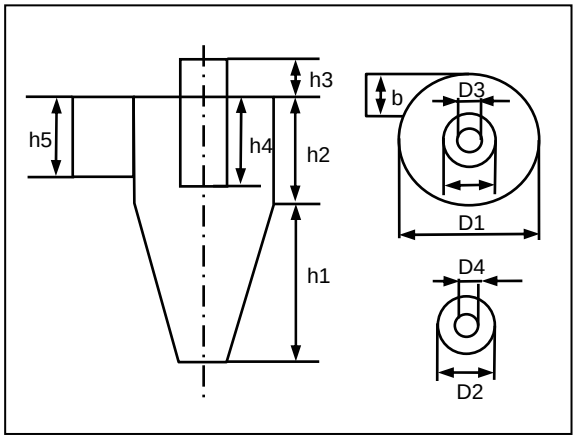

Figure 2: Schematic diagram of the cyclone's geometry.

h1	h2	h3	h4	h5
400	340	50	170	160
D1	D2	D3	D4	b
300	120	60	60	70

Table 1: Geometric dimensions given in *mm*.

Once started the discrete particles can (a) escape at the annulus outlet at the top of the vortex finder, (b) be collected at the cyclone's bottom exit or (c) re-enter the particle strand. In the latter case the particle trajectories are aborted.

In the case of a highly laden gas-solid cyclone the EuEuLa model is believed to handle both, the particle strand formation at the wall by the basic EuEu simulation as well as the inner particle vortex separation by the EuLa model. While the first phenomenon is based on a mean particle diameter the latter mechanism is easily further detailed by considering different particle classes.

RESULTS – HIGHLY LADEN CYCLONE

All numerical simulations were performed with the commercial CFD package Fluent (2003) on a Linux cluster.
The cyclone considered is sketched in Figure 2 with dimensions listed in Table 1. The computational domain has been discretized by a hexahedral grid with approximately 130,000 cells.

Furthermore, all calculations are performed unsteady with fixed time-steps of 0.001s. During the simulation characteristic values like the collection efficiency are monitored in order to check if the spin-up process is completed.

At the cyclone inlet the integral particle mass-loading at the cyclone's inlet is set to 10 kg/kg. The normal gas and particle velocities are set to 15 m/s respectively. At the cyclone gas outlet a centric disk prevents reversed gas flow. In the annulus region gas and particles can freely leave the cyclone.

At the lower dust outlet the arriving particles are removed by a sink term S_s in the solid's mass conservation equation. Analogously, the corresponding particle momentum has to be eliminated by the sink $\boldsymbol{S}_s$.

EuEu Results

Due to its enormous computational costs only mono-disperse particles are considered with the EuEu model. In Table 2 the considered particle classes are listed.

diameter	2 μm	5	10	20	100
percentage	5 %	15	40	30	10

Table 2: Particle spectrum at cyclone inlet.

The computational results show a quite different particle separation behaviour in dependence of the mean particle diameter. In case of large particles with a mean diameter of 100 μm the particles are separated mainly by gravitational forces. Thereby, the particle strand at the wall even does not complete a full rotation. In Figure 3 the corresponding particle strand formation at the wall is depicted. The particle separation efficiency tends towards one thus, all particles are collected. This agrees with Muschelknautz's (1972) theory which predicts that particle collection is governed by the separation of the wall near particle strand.

In the case of 20 μm particles the gravitational acceleration is less important. Once again the particles are forming a wall near strand but in this case the strand is circulating several times before the particles are collected at the bottom of the cyclone. This behaviour is depicted in Figure 4. Also in this case a very high particle volume fraction of $\alpha_s > 0.6$ occurs in the particle strand regions.

In contrast to that no significant strand formation can be observed in case of very small particles. Considering particle diameters of 2 μm the simulated maximum solid volume fraction reaches only about 15 %. This disagrees with Muschelknautz's theory which predicts a particle strand formation for every particle class.

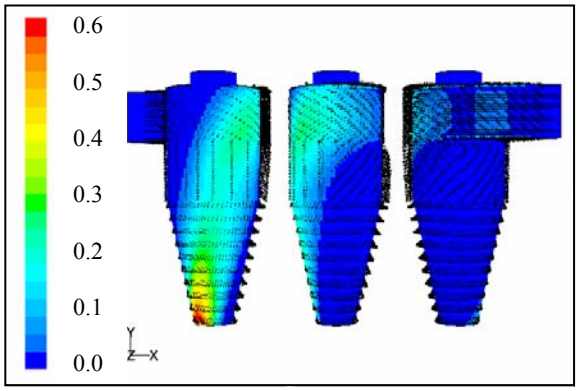

Figure 3: Wall-near particle volume fraction as a result of a EuEu mono-disperse 100 μm particle simulation

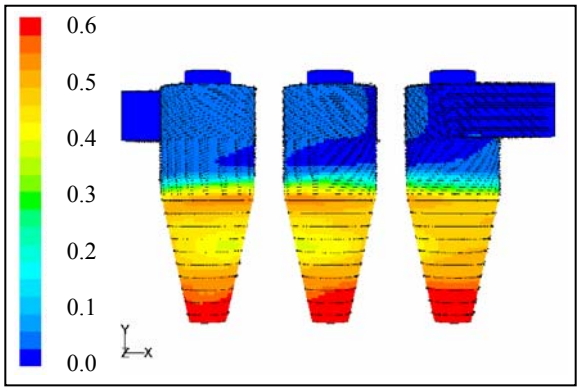

Figure 4: Wall-near particle volume fraction as a result of a EuEu mono-disperse 20 μm particle simulation

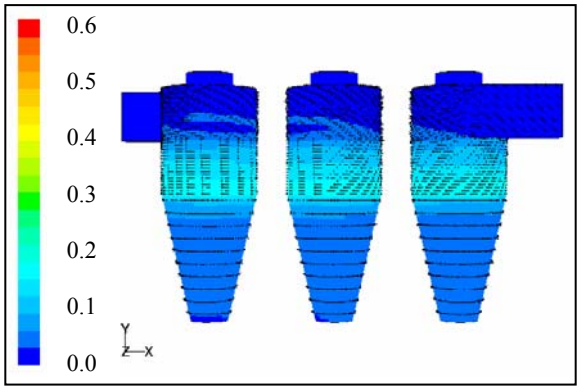

Figure 5: Wall-near particle volume fraction as a result of a EuEu mono-disperse 2 μm particle simulation

All of the simulations show a great sensitivity with respect to the order of the discretization scheme. In Figure 6 a profile of the gas tangential velocity is given in a horizontal observation line just below the vortex finder. If a first order discretization scheme is used the vortex motion is partly suppressed by numerical diffusion. Thus the maximum tangential velocity is much lower than in the case of a second order discretization.

In accordance to the differences in the vortex motion the particle separation efficiency also significantly depends on the discretization scheme. In Table 3 the overall particle collection efficiencies are listed.

diameter	2 μm	5	10	20	100
$\eta_{EuEu,O1}$	0.01	0.22	0.47	0.97	1.00
$\eta_{EuEu,O2}$	0.41	0.64	0.83	0.98	1.00

Table 3: Particle collection efficiencies η as result of mono-disperse EuEu simulations using a first order (O1) and second order (O2) discretisation scheme.

EuLa Results

In case of a high particle mass-loading the EuLa model exhibits a very difficult convergence behaviour. The momentum exchange field has to be updated every five iterations in order to avoid numerical divergence. Thus, the simulation times of the EuLa model are longer than for a mono-disperse EuEu simulation.

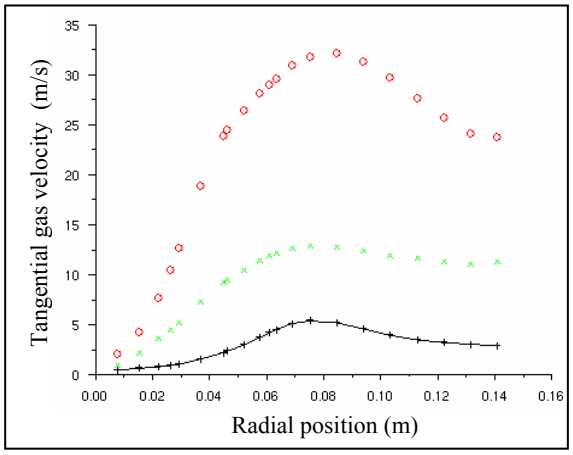

Figure 6: Profile of tangential gas velocity at a horizontal line just below the vortex finder as result of EuLa (plus symbol) as well as first (cross) and second (circle) order EuEu simulations.

The standard EuLa model does not account for a reduced integral drag force of a particle strand. Ignoring the presence of other particles the drag force of every single particle acts on the continuous gas phase. Thereby, the retarding force of the multitude of particles in the wall near region is over-predicted. As a result the inner vortex motion is strongly suppressed as depicted in Figure 6.

diameter	2 μm	5	10	20	100
EuLa	0.16	0.19	0.38	0.94	1.00
EuEuLa	0.43	0.76	0.82	0.98	1.00

Table 4: Particle collection efficiencies η as result of poly-disperse EuLa and EuEuLa simulations representing an overall collection efficiency of η_{tot} = 0.57 and 0.86 respectively.

The reduced vortex motion is responsible for a low overall particle collection efficiency given in Table 4.

EuEuLa Results

The EuEuLa model is based on an EuEu simulation with mono-disperse 20 μm particle. In a second step poly-disperse particles according to the particle spectrum given

in Table 2 emit at the RSL. Figure 7 depicts the position of the RSL at α_s = 0.01 while Figure 8 shows characteristic particle tracks in the cyclone's core region.

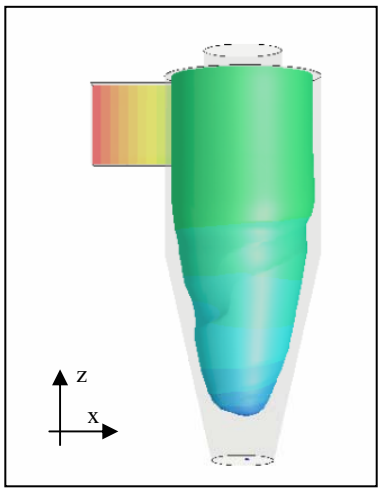

Figure 7: Re-suspension layer (RSL) coloured by its radial coordinate of r = 0 (blue) to 20 (red) mm.

Table 4 indicates that the global particle collection can be predicted reasonably by the EuEuLa model. The global particle strand separation is captured by the EuEu simulation while the inner vortex separation of the particle classes is handles by EuLa simulations.

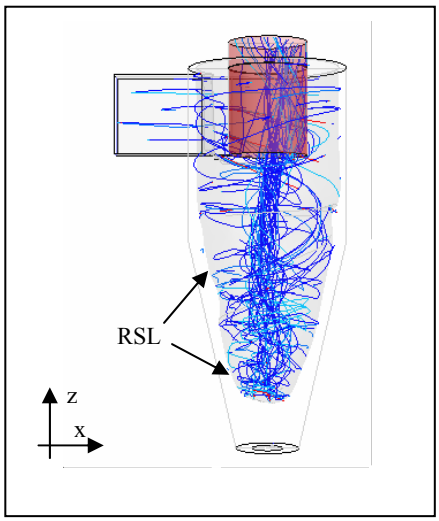

Figure 8: Characteristic particle paths in the inner core region coloured by particle diameter of (red) 100 µm to (blue) 2 µm.

In terms of computation times the EuEuLa model is by far the most efficient of the three models presented in this paper. Furthermore, it is the only model that captures both the particle strand formation as well as the distinct collection efficiencies of different particle classes.

CONCLUSION

Three different simulation approaches, namely the EuEu continuum model and the EuLa discrete particle model as well as a combining EuEuLa model, are applied for the simulation of highly laden gas-solid cyclone operation.

First EuEu simulation results indicate that in wall near regions particle volume fractions are high and therefore particle-particle interactions are important. In contrast to that the standard EuLa model neglects the presence of other particles. As a consequence the integral retarding force of the multitude of particles is over-predicted and the inner vortex motion is suppressed.

The proposed combining EuEuLa approach incorporates both the particle strand behaviour in the wall near region as well as the distinguishing particle class separation in the inner core region.

On principal the EuEuLa model works numerically stable and produces reasonable results. In terms of computational efforts the EuEuLa model is in the range of a EuEu mono-disperse simulation while it is cheaper than a poly-disperse EuLa simulation.

The authors believe that the EuEuLa model could offer an efficient alternative for simulating highly laden cyclones. Nevertheless, at this point the method is only in a proposal state and results have to be further checked with respect to grid dependencies, different mass loadings and so on. After all simulations results should be compared to measurements that are planned in the near future.

ACKNOWLEDGEMENT

This R&D work has been partly funded by the Austrian Ministry for Economy and Labour in the frame of its Industrial Competence Centre Program "Knet MET". The authors are grateful for this funding.

REFERENCES

DALLA DALLA J. M., (1948), "Micromerics", *Pitman*, London.

FLUENT (2003), "Fluent User Guide", *Fluent Inc.,* Lebanon, USA.

GARSIDE J. and AL'DIBOUNI M.R., (1977), "Velocity-Voidage Relationships for Fluidization and Sedimentation", *I&EC Process Des. Dev.*, **16**, 206-214.

GIDASPOW D., (1994), "Multiphase Flow and Fluidization", *Academic Press*, San Diego, US.

MORSI S. A. and ALEXANDER A. J., (1972), "An Investigation of Particle Trajectories in Two-Phase Flow Systems", *J.Fluid.Mech.*, **55(2)**, 193-208.

MUSCHELKNAUTZ E., (1972), "Die Berechnung von Zykonabscheidern für Gase", *Chem.-Ing.-Techn.*, **Nr.1+2**, 63-71.

SLACK M. et al. (2003), "Reynolds Stress Model for Eulerian Multiphase", *Symp. on Turbulence Heat and Mass Transfer*, Begell House Inc., 1047-1054.

SOMMERFELD M., (1996), "Modellierung und numerische Berechnung partikelbeladener turbulenten Strömungen", *Shaker*, Aachen, Deutschland.

SYAMLAL M. and O'BRIAN T. J., (1989), "Computer Simulation of Bubbles in a Fluidized Bed", *AIChE Symp. Series*, **85,** 22-31.

SYAMLAL M., ROGERS W. and O'BRIAN T. J., (1993), "MFIX Documentation", *National Technical Information Service*, Springfield, US.

ZWINGER T., (2000), "Dynamik einer Trocken-schneelawine auf beliebig geformten Berghängen", *Dissertation*, Wien, Austria.